Arylpiperazines with Serotonin-3 Antagonist Activity: A Comparative Molecular Field Analysis

Antonio Morreale,[†,‡] Enrique Gálvez-Ruano,[‡] Isabel Iriepa-Canalda,[‡] and Donald B. Boyd*,[†]

Department of Chemistry, Indiana University−Purdue University at Indianapolis (IUPUI), 402 North Blackford Street, Indianapolis, Indiana 46202-3274, and Departamento de Química Orgánica, Universidad de Alcalá de Henares, E-28871 Alcalá de Henares, Spain

Comparative molecular field analysis (CoMFA) is applied to antagonists of the 5-HT$_3$ receptor. Analysis is done separately on three published sets of arylpiperazines and on a combination of the three sets. *d*-Tubocurarine, a conformationally restricted 5-HT$_3$ ligand, is used as a template to assist in selecting the conformation of the antagonists for CoMFA alignment. Two forms of the arylpiperazines (neutral and protonated) and three different kinds of calculated charges (Gasteiger−Hückel, AM1, and AM1 with solvation effect included) are compared. Protonated structures give better statistical results than the neutral species. The way in which charges are calculated does not greatly affect the results. In terms of molecular fields, the behavior in each separate set of compounds cannot be extrapolated to the combined set of 47 compounds. The average value of r^2_{cv} from PLS cross-validation on the combined set is 0.70 and varies between 0.56 and 0.80 depending on the orientation of the molecules in the coordinate system. The CoMFA model is tested on four compounds not in the training set: quipazine, *N*-methylquipazine, 4-phenyl-*N*-methylquipazine, and KB-6933. Mean agreement of experimental and predicted pK_i values of the antagonists is 0.7 log unit. Novel structural modifications are interpreted by the CoMFA model.

Introduction

Of the many subtypes of serotonin (5-hydroxytryptamine) receptors, 5-HT$_3$ is rather unique. The other serotonin receptors are G-protein-coupled, whereas 5-HT$_3$ is a ligand-gated ion channel in neurons.[1] No three-dimensional structure of the 5-HT$_3$ receptor is available, but many high-affinity, selective ligands have been discovered using traditional medicinal chemistry strategies and using molecular modeling.

Over the last 10−15 years, pharmacology has contributed to an understanding of the 5-HT$_3$ receptor's mediation in conditions and diseases of the central nervous system. Chemotherapy's troublesome side effects of nausea and vomiting can be rapidly ameliorated by administration of 5-HT$_3$ antagonists. Three of these pharmaceutical agents have been introduced into medical practice: ondansetron[2] (1990; **1**), granisetron[3] (1991; **2**), and tropisetron[4] (1992; **3**) (Figure 1). Research on 5-HT$_3$ receptor antagonists continues[5] because of potential uses in the treatment of psychosis, anxiety, migraine, schizophrenia, pain, substance abuse, and memory impairment. Some of the other well-studied antagonists include zatosetron (**4**),[6] bemesetron (**5**),[7] ramosetron (**6**),[8] azasetron (**7**),[9] itasetron (**8**),[10] cilasetron (**9**),[11] zacopride (**10**),[12] lerisetron (**11**),[13] and alosetron (**12**).[14]

Substantial progress has been made in understanding the 5-HT$_3$ pharmacophore, but due to a broad diversity in ligand structures, questions remain for some of the newer structural classes. A good review about chemical structures and proposed pharmacophores can be found in the book of King, Jones, and Sanger.[15] Perhaps the most well-known 5-HT$_3$ pharmacophore is the one proposed by Hibert.[16] It consists of three components (**13**): (1) an aromatic ring, (2) a carbonyl-containing linking moiety, and (3) an out-of-plane basic center. These components have a rather specific spatial arrangement.
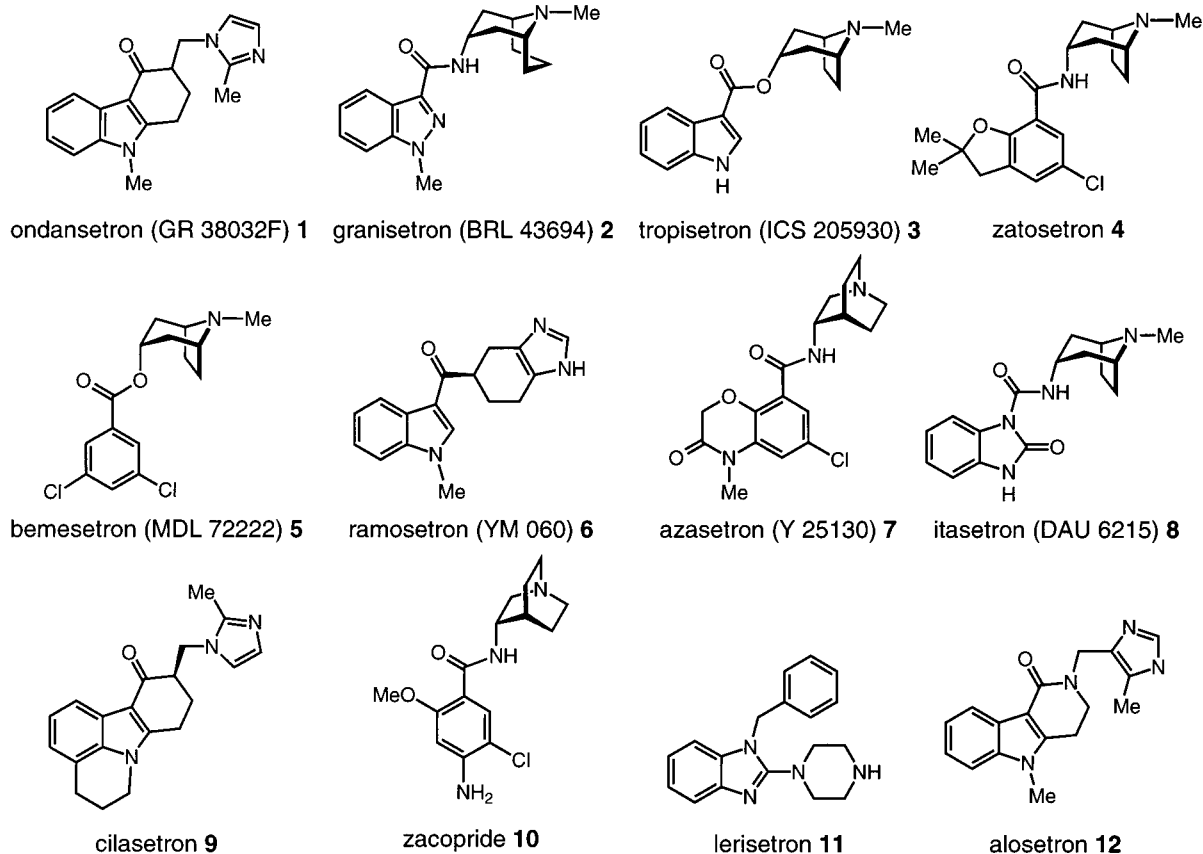

13
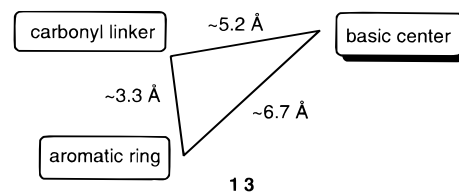
Since Hibert published his model in 1990, a number of refinements and extensions to this model have been proposed.[17−21] As additional compounds have been synthesized and reported, it became recognized that the pharmacophoric requirements were broader than initially envisioned. The second component of the pharmacophore, the carbonyl moiety, is not essential for high affinity.[22] This component can be better defined as a hydrogen-bonding region. One of the newer 5-HT$_3$ ligands that helps define the pharmacophoric requirements is quipazine (**14**), which exhibits 5-HT$_3$ antagonist properties[23] as well as agonist character in some preparations.[24] Although quipazine lacks a carbonyl group, the negative electrostatic potential energy field generated by the quinoline nitrogen may resemble that generated by a carbonyl group.[19] Indeed, Hibert et al.[16]

* Address correspondence to Prof. D. B. Boyd. Tel: (317) 274-6891. Fax: (317) 274-4701. E-mail: boyd@chem.iupui.edu.
† Indiana University−Purdue University at Indianapolis.
‡ Universidad de Alcalá de Henares.

ondansetron (GR 38032F) **1**   granisetron (BRL 43694) **2**   tropisetron (ICS 205930) **3**   zatosetron **4**

bemesetron (MDL 72222) **5**   ramosetron (YM 060) **6**   azasetron (Y 25130) **7**   itasetron (DAU 6215) **8**

cilasetron **9**   zacopride **10**   lerisetron **11**   alosetron **12**

Figure 1. Examples of potent 5-HT$_3$ receptor antagonists.

anticipated that the lone pair of the quipazine nitrogen may play a role equivalent to the carbonyl oxygen.

14
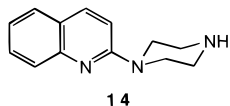
The discovery of quipazine has stimulated much interest in additional arylpiperazines as a new class of 5-HT$_3$ antagonists.[13,25−31] Whereas quipazine itself binds to several serotonin receptors, some of the newer members of this class are highly selective 5-HT$_3$ antagonists.
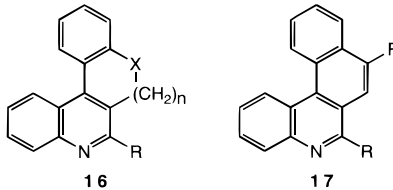
Beyond molecular modeling associated with the well-studied three-component pharmacophore model, quantitative structure−activity relationship (QSAR) analyses of 5-HT$_3$ ligands have been difficult and few have been published. One particularly successful QSAR study[19] on 5-HT$_3$ antagonists reported using three novel computed descriptors: (1) a distance between a lipophilic region generated by the aromatic ring and a hydrophilic area near the basic nitrogen or center, (2) the maximum value of the lipophilic field, and (3) the maximum value of the negative electrostatic field near the carbonyl group. Unfortunately, in their multiple regression analysis the authors omitted, without explanation, several antagonists that they mention in their paper; also the authors did not reveal details of how the distance was measured. Nevertheless, a very respectable QSAR equation with r^2 equal to about 0.8 was obtained.

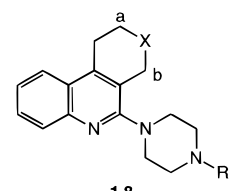Techniques for determining three-dimensional quantitative structure−activity relationships (3D-QSAR) in general,[32,33] and comparative molecular field analysis (CoMFA),[34−36] in particular, have proven useful in understanding the biological activities of compounds. To date, over 200 applications of CoMFA to various types of bioactive compounds have been published. For a set of related chemical structures, CoMFA has a demonstrated ability to find steric and electrostatic features that differentiate their bioactivities. In some cases, CoMFA and traditional QSAR (Hansch) models can be rationalized with respect to each other. In other cases, a CoMFA model can be found where the traditional (Hansch) approach fails. Valid CoMFA models, if established, can be used to screen design ideas for new structures within or close to the compound space spanned by the training set.

To the best of our knowledge, only two prior CoMFA studies have been published on 5-HT$_3$ receptor ligands.[37] One involved a set of 39 partial agonists in a series of pyrrolothienopyrazines giving r_{cv}^2 as high as 0.46.[20] The other prior study is more germane to the work here and involved a set of 24 antagonists.[29] The compounds were arylpiperazines with four fused rings. The CoMFA analysis, giving r_{cv}^2 of ca. 0.7, was tested only on Gasteiger−Marsili partial atomic charges derived from electronegativities. Although Anzini et al.[28] wrote that their CoMFA model had good predictive capacity, they did not test it on any structures not in their training set. Also they were careful to warn that the molecules in their study were so similar to each other that their CoMFA model may not be broadly applicable.

Here we undertake a larger analysis on 47 arylpiperazines consisting of the 24 compounds from the Anzini et al.[29] paper plus compounds from two additional

Table 1. Benzofuro[2,3-*c*]quinoline, Benzo[*k*]phenanthridine, and Related Piperazinyl 5-HT$_3$ Receptor Antagnists of Anzini et al.[29]
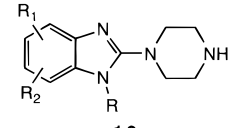
compd	X	n	R	R′	pK_i
16a	O	0	−N(C$_2$H$_4$)$_2$NH		7.49
16b	O	0	−N(C$_2$H$_4$)$_2$N−CH$_3$		7.90
16c	O	0	−N(C$_2$H$_4$)$_2$N−C$_2$H$_5$		7.28
16d	O	0	−S(C$_2$H$_4$)N(CH$_3$)$_2$		6.39
16e	O	1	−N(C$_2$H$_4$)$_2$NH		7.94
16f	O	1	−N(C$_2$H$_4$)$_2$N−CH$_3$		8.80
16g	O	1	−N(C$_2$H$_4$)$_2$N−C$_2$H$_5$		7.27
16h	O	1	−S(C$_2$H$_4$)N(CH$_3$)$_2$		5.00
16i	O	2	−N(C$_2$H$_4$)$_2$NH		7.91
16j	O	2	−N(C$_2$H$_4$)$_2$N−CH$_3$		8.42
16k	O	2	−N(C$_2$H$_4$)$_2$N−C$_2$H$_5$		7.84
16l	O	2	−S(C$_2$H$_4$)N(CH$_3$)$_2$		7.34
16m		2	−N(C$_2$H$_4$)$_2$NH		8.27
16n		2	−N(C$_2$H$_4$)$_2$N−CH$_3$		8.46
16o		2	−N(C$_2$H$_4$)$_2$N−C$_2$H$_5$		8.10
16p		2	−S(C$_2$H$_4$)N(CH$_3$)$_2$		5.00
17a			−N(C$_2$H$_4$)$_2$NH	H	6.88
17b			−N(C$_2$H$_4$)$_2$N−CH$_3$	H	8.02
17c			−N(C$_2$H$_4$)$_2$N−C$_2$H$_5$	H	7.79
17d			−S(C$_2$H$_4$)N(CH$_3$)$_2$	H	5.00
17e			−N(C$_2$H$_4$)$_2$NH	OCH$_3$	7.18
17f			−N(C$_2$H$_4$)$_2$N−CH$_3$	OCH$_3$	7.38
17g			−N(C$_2$H$_4$)$_2$N−C$_2$H$_5$	OCH$_3$	6.65
17h			−S(C$_2$H$_4$)N(CH$_3$)$_2$	OCH$_3$	5.00

Table 2. 3- and 4-Substituted-2-(1-piperazinyl)quinoline 5-HT$_3$ Receptor Antagonists of Castan et al.[30]

| compd	X	R	pK_i
18a	direct bond a−b	CH$_3$	10.15
18b	CH$_2$	H	10.00
18c	CH$_2$	CH$_3$	10.01
18d	S	CH$_3$	9.40
18e	CH$_3$N	CH$_3$	8.50
18f	no bond a−b	CH$_3$	9.27

papers: Castan et al.[30] and Orjales et al.[13] The structures in these three sets are shown in Tables 1−3. For convenience, in the remainder of this paper, we will refer to these three as the A, C, and O sets, respectively. Additional sets of compounds were sought for inclusion in our analysis, but either no comparable biological data were available for them or the structures were too dissimilar to include.

As is well-known, the alignment of the molecules is key to obtaining a meaningful CoMFA. As the flexibility of the molecules increases, more possibilities for alignment exist. A rigid template is always desired for this reason. It can be seen in Tables 1−3 that the compounds have relatively few rotatable bonds, but a template that could help pin down the few remaining degrees of freedom would be useful.[1] *d*-Tubocurarine

Table 3. Piperazinylbenzimidazole 5-HT$_3$ Receptor Antagonists of Orjales et al.[13]

compd	R	R$_1$	R$_2$	pK_i
19a	CH$_3$	H	H	7.3
19b	CH$_2$CH$_3$	H	H	7.1
19c	(CH$_2$)$_2$CH$_3$	H	H	8.0
19d	cyclo-C$_3$H$_5$	H	H	8.8
19e	CH$_2$Ph	H	H	9.2
19f	CH$_2$Ph	(5)F	H	9.5
19g	CH$_2$Ph	(5)Cl	H	9.5
19h	CH$_2$Ph	(5)CH$_3$	H	8.8
19i	CH$_2$Ph	(5)CH$_3$O	H	7.2
19j	CH$_2$Ph	(5)OH	H	9.5
19k	CH$_2$Ph	(6)CH$_3$O	H	8.4
19l	CH$_2$Ph	(6)OH	H	9.0
19m	CH$_2$Ph	(4)CH$_3$O	H	6.7
19n	CH$_2$Ph	(7)CH$_3$O	H	9.4
19o	CH$_2$Ph	(5)CH$_3$	(6)CH$_3$	8.7
19p	CH$_2$Ph	(5)Cl	(6)Cl	8.5
19q	H	H	H	7.5

(**15**) was chosen as a template because (1) it has been reported to reversibly block the 5-HT$_3$ receptor,[38−40] (2) the three-dimensional structure is known from X-ray crystallography,[41] and (3) the conformation is relatively rigid. We assume that the 5-HT$_3$ ligands share a common structural framework in their interactions with the receptor.[1] Using this template, we can envisage a bioactive conformation for the ligands of the 5-HT$_3$ receptor as detailed in the next section.
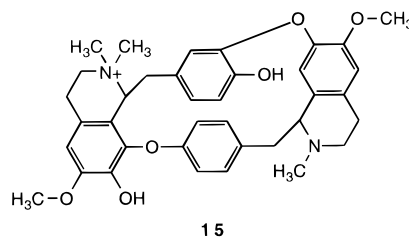
Computational Methods

The starting molecular structure for *d*-tubocurarine was obtained from a published X-ray crystallographic study.[37] An assessment of the conformational flexibility of *d*-tubocurarine is presented in Figure 2. The SYBYL molecular modeling package[42] and the TRIPOS force field[43] were used to sample conformational space[44] starting from the crystallographic geometry. Ten picoseconds of molecular dynamics were run. As can be seen in the figure, the basic conformation of the macrocycle does not change significantly. During the simulation, the side chains flex and the plane of one phenyl ring tips with respect to the solid-state conformation. The rest of the structures overlap well.

Because the X-ray study of *d*-tubocurarine was done to standards of a quarter century ago (final *R* value of only 9.1%), the structure was first optimized by semiempirical molecular orbital calculations using the AM1 Hamiltonian[45] as implemented in MOPAC.[46]

The 47 antagonists were built with Quanta/CHARMm software, a commercially available molecular modeling program.[47] Standard bond lengths and angles were used. With the CHARMm force field[48,49] and partial atomic charges, the molecular geometries of *d*-tubocurarine and the antagonists were each separately energy-minimized using the adopted-
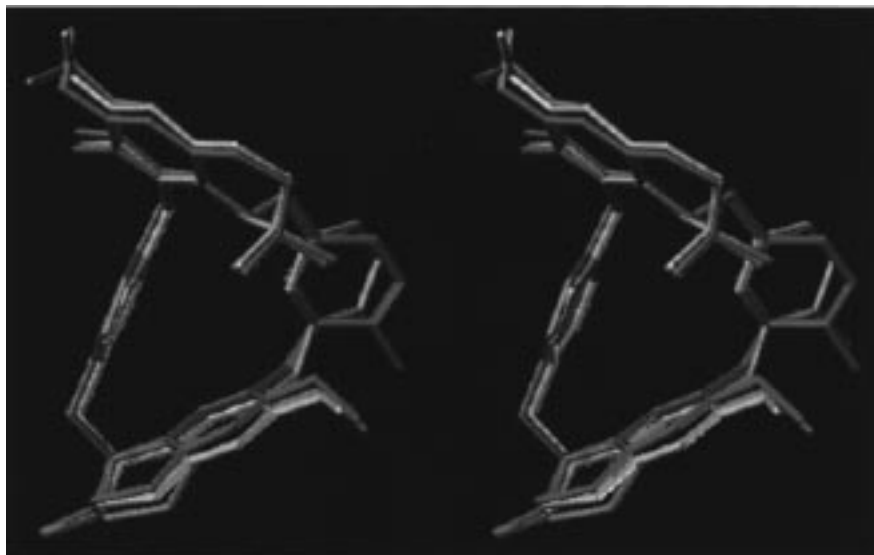
Figure 2. Relaxed stereoview of the conformations of *d*-tubocurarine obtained from a short molecular dynamics simulation. The monomethylated nitrogen was treated as protonated. Because hydrogens can be poorly located by X-ray diffraction, these atoms were added with standard bond lengths and angles using SYBYL. However, the hydrogens are not shown in this figure to make the framework atoms easier to see. The simulation was done with defaults in SYBYL, i.e., with a step size of 1 fs, at 300 K, and without charges or solvent. Structures from the trajectory were subjected to 300 steps of default energy minimization. The starting X-ray structure is in white, and the energy-minimized structures after 3 and 10 ps of dynamics are shown in orange and cyan, respectively. The dimethylated nitrogen is near the center foreground. The monomethylated nitrogen is at the bottom left of the figure.
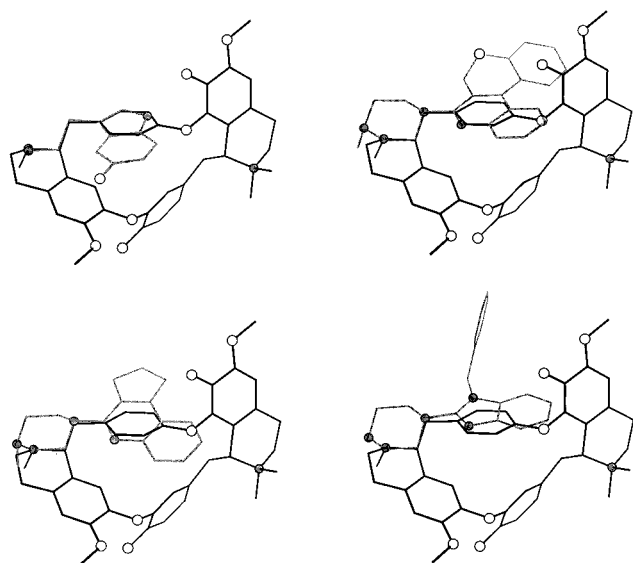
Figure 3. Superposition of *d*-tubocurarine (black) with 5-HT$_3$ ligands (gray). Upper left: serotonin. Upper right: **16f**. Lower left: **18a**. Lower right: **19e**. Open circles represent oxygen atoms, shaded circles are nitrogens, and the rest are carbon atoms. Hydrogens are omitted for clarity.

based Newton–Raphson and a convergence criteria of 0.01 kcal/mol (energy difference between iterations).

Next each 5-HT$_3$ antagonist (Tables 1–3) was manually aligned on the *d*-tubocurarine model. The superimposition was based on a serotonin-like substructure embedded in *d*-tubocurarine. This substructure was selected based on molecular modeling and overlap of optimized serotonin and *d*-tubocurarine structures. The alignment of an AM1-optimized model of serotonin itself with the embedded substructure of *d*-tubocurarine can be seen in Figure 3, which also shows the resemblance between the most active compound in each of the three sets and the target substructure of *d*-tubocurarine.

The aligned conformations were ported from Quanta to SYBYL for CoMFA analysis. In SYBYL, the molecules were

reoptimized with the TRIPOS force field using the default conjugate gradient algorithm,[50] a convergence criterion in the energy gradient of 0.001 kcal/(mol Å), and as recommended, charges were not included in the energy evaluations.[43] These further energy minimizations did not substantially alter the conformations but did help guarantee that the aligned 5-HT$_3$ ligands are strictly comparable.

We present results corresponding to six separate CoMFA runs: each antagonist was calculated in its neutral state and in the protonated state, and charges were computed by three different methods (see below). In the protonated species the proton was added to the distal nitrogen of the piperazine ring. These six protocols were applied to each of the three sets and to the combined set.

CoMFA Set Up. 1. Alignment of the Molecules. Using the conformations derived from *d*-tubocurarine, the individual 5-HT$_3$ antagonists were multifitted together to achieve an alignment appropriate for CoMFA. Multifitting is an algorithm for flexibly fitting two or more molecules together so that paired atoms in different molecules are brought as close together as possible subject to the constraint of keeping the molecular mechanics energy of the molecules low.[51] The SYBYL multifitting procedure was used without charges and with a force constant[52] of 5 kcal/(mol Å^2) between paired atoms.

Atoms selected for multifitting were as follows. In the A set, we used all nonhydrogenic atoms shown explicitly in **20**, so both the piperazine-containing compounds and the acyclic thiols, such as **16d**, **17d**, etc., could be aligned in an analogous way. In the C set, we used all atoms (except hydrogens) in the quinoline and piperazine rings. In the O set, we picked all the atoms (except hydrogens and substituents) in the benzimidazole and piperazine rings. For the combined set of 47 compounds, we used the six carbon atoms of the phenyl ring, a nitrogen in the fused aromatic ring, and the five atoms in the piperazinyl or sulfur-containing side chain. The multifitting operations in SYBYL were automated with SYBYL programming language (SPL) scripts. Figure 4 shows a stereoview of the combined set of 47 molecules in their final alignment used in CoMFA.

2. Calculation of the Atomic Charges. Partial atomic charges were calculated using three different methods: (1) empirical Gasteiger–Hückel, (2) single-point (no further geometry optimization) semiempirical molecular orbital calcula-
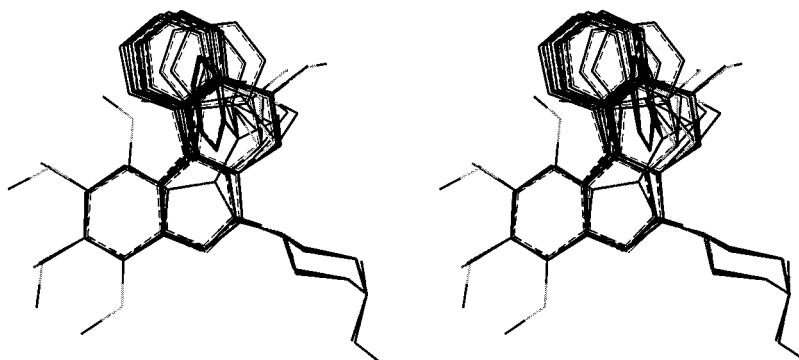
Figure 4. Relaxed stereoview of the 47 compounds aligned as used in the CoMFA calculations.

20, X = N, S
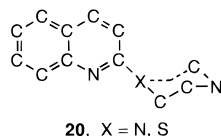
tions with the AM1 model, and (3) single-point AM1 with the effect of an aqueous environment included through the solvation model 2 (SM2) continuum model.[53] With both semiempirical methods, the point charges were those derived from fitting the electrostatic potential energy surface as generated in the Spartan molecular modeling program.[54] The semiempirical charges, being dependent on molecular geometry, were calculated on the final structures after the multifitting alignment was performed.[55] Although atomic partial charges are not physical observables and electrostatically fit charges have their inherent uncertainties,[56] one would expect "quality" to increase in the order (1) < (2) < (3).[57]

3. CoMFA Lattice. Each of the sets of the overlapped molecules was surrounded by a 3D grid of points (810 for the A set, 900 for the C set, 800 for the O set, and 1089 for the combined set) regularly spaced at 2 Å (the default setting in SYBYL) in the three dimensions extending at least 4 Å beyond the union volume occupied by the superimposed molecules. The probe used to compute the CoMFA steric and electrostatic fields was the default sp³ carbon atom with a +1 charge. The energies at each grid point were determined with the TRIPOS force field. Cutoff values for both fields were set to the default: 30 kcal/mol.

4. Partial-Least-Squares Calculations. PLS[58−60] was performed separately on each of the three sets and on the combined set. The standard leave-one-out (LOO) cross-validation technique was applied to obtain the optimum number of components (ONC). In addition, CoMFA models were computed using the ONC but without cross-validation. Better results were obtained without scaling the grid point values, but the results reported in this paper used the standard scaling option in SYBYL. Column filtering (minimum σ) was used at the default value of 2 kcal/mol in the cross-validation part.

5. Statistics. As usual, the merit of the CoMFA models was judged on the basis of the cross-validated r_{cv}^2 (also called q^2 by some authors), PRESS (sum of squared deviations between predicted and actual property values for all N molecules in each set), and SEE (standard error of estimate).[33]

6. Biological Activities. Binding constants K_i (in molar units) were obtained from the literature.[13,29,30] The assays involved measuring displacement of a radioligand from the 5-HT₃ receptor. For purposes of the CoMFA analyses, the bioactivity data were converted to pK_i values.

Results

Anzini et al. Set (A Set). The ONC is 5 for all the six CoMFA models (Table 4) involving set A. The three models for protonated species (models 1−3) show higher r_{cv}^2 values and lower PRESS values than for the neutral

ones (models 4−6). The r_{cv}^2 values approach 0.8, whereas Anzini et al.[29] for the same set of structures obtained 0.70−0.72, depending on the coordinate system of the grid. The improvement in r_{cv}^2 is presumably due mainly to better alignment and conformations. In comparing the columns in Table 4, the method of computing charge makes little difference with either the protonated or neutral models. Non-cross-validated parameters (r^2 and SEE) are better for protonated systems than for neutral ones, but similar within each group. The main difference between models 1−3 and models 4−6 (Table 4) is in the relative contribution of the fields. The CoMFA models for the protonated species (1−3) show a high contribution (ca. 82%) of the steric field (SF) compared to the electrostatic field (EF) (ca. 18%). With the neutral molecules (models 4−6), the picture is more complex: Gasteiger−Hückel charges give a much lower contribution from the SF (39%) than the AM1/SM2 charges (91%).

Castan et al. Set (C Set). None of the CoMFA models (Table 5) are good: r_{cv}^2 is below 0.2 in all six cases. Neither the type of charges nor the state of protonation is able to give a good model. The non-cross-validated r^2 is as high as 0.8.

Orjales et al. Set (O Set). The CoMFA models (Table 6) are not as strong as with the A set, but at least the r_{cv}^2 values for the protonated species (models 1−3) are above the threshold[61] (0.3) for ruling out chance correlation. There is no pattern of improvement in r_{cv}^2 due to the way of calculating charges, and the non-cross-validated r^2 remains almost constant for all six models. The steric contribution is more important with the protonated species (models 1−3) than the neutral ones (models 4−6).

Combined Set. For the set of 47 molecules, the values of r_{cv}^2 are quite good, being above 0.6 in all cases (Table 7). The non-cross-validated r^2 is over 0.9 in several cases. Models 2 and 3 give an ONC of 3. It has been proposed that one might expect three components should be enough to explain the results in a respectable CoMFA study.[33] The statistical parameters do not change much as the complexity in the charge calculation method increases or in going from protonated to neutral species. The steric contribution of the CoMFA models is consistently above 90% for the protonated species and around 60−65% for the neutral ones.

A plot of predicted (using model 3 of Table 7) vs actual values of pK_i for the 47 compounds is shown in Figure 5. Also plotted is the evolution of PRESS and r_{cv}^2 values as the number of extracted components increases. As

Table 4. CoMFA Models Obtained for 24 Compounds in Set A (Anzini et al.[29])[a]

	model 1[b]	model 2[c]	model 3[d]	model 4[e]	model 5[f]	model 6[g]
ONC	5	5	5	5	5	5
r^2_{cv}	0.745	0.781	0.771	0.562	0.533	0.614
PRESS	0.664	0.616	0.629	0.870	0.899	0.864
SEE	0.380	0.362	0.356	0.438	0.442	0.383
r^2	0.917	0.924	0.927	0.889	0.887	0.924
F ($n_1 = 5$, $n_2 = 18$)	39.610	43.836	45.428	28.893	28.260	99.826
P ($r^2 = 0$, $n_1 = 5$, $n_2 = 18$)	0.000	0.000	0.000	0.000	0.000	0.000
SF contribution	83.2%	83.3%	82.0%	39.0%	57.5%	91.2%
EF contribution	16.8%	16.7%	18.0%	61.0%	42.5%	8.8%

[a] ONC, optimum number of components; PRESS, predictive sum of squares; SEE, standard error of estimate; r^2, amount of variance explained; F, fraction of explained versus unexplained variance; P, the probability that the observed F-ratio will be obtained by chance alone, if the target and explanatory variables are truly uncorrelated (i.e., P is the probability that the null hypothesis is satisfied); SF, steric field; EF, electrostatic field. [b] Protonated structures with Gasteiger−Hückel partial atomic charges. [c] Protonated structures with AM1 charges. [d] Protonated structures with AM1/SM2 charges. [e] Neutral structures with Gasteiger−Hückel charges. [f] Neutral structures with AM1 charges. [g] Neutral structures with AM1/SM2 charges.

Table 5. CoMFA Models Obtained for 6 Compounds in Set C (Castan et al.[30])[a]

	model 1	model 2	model 3	model 4	model 5	model 6
ONC	2	1	1	2	1	1
r^2_{cv}	0.137	0.059	0.059	0.180	−0.002	0.007
PRESS	0.871	0.867	0.867	0.849	0.894	0.890
SEE	0.437	0.617	0.617	0.396	0.581	0.580
r^2	0.783	0.523	0.523	0.821	0.577	0.579
F ($n_1 = 2$, $n_2 = 10$)	18.003	12.047	12.082	23.005	14.998	15.143
P ($r^2 = 0$, $n_1 = 2$, $n_2 = 10$)	0.003	0.005	0.005	0.000	0.003	0.003
SF contribution	94.7%	95.4%	95.1%	59.9%	68.9%	68.1%
EF contribution	5.3%	4.6%	4.9%	40.1%	31.1%	31.9%

[a] See Table 4 for definition of symbols.

Table 6. CoMFA Models Obtained for 17 Compounds in Set O (Orjales et al.[13])[a]

	model 1	model 2	model 3	model 4	model 5	model 6
ONC	5	5	5	5	5	3
r^2_{cv}	0.523	0.349	0.368	0.041	0.136	0.103
PRESS	0.786	0.918	0.905	1.114	1.058	0.981
SEE	0.173	0.172	0.172	0.199	0.171	0.284
r^2	0.977	0.977	0.977	0.970	0.977	0.926
F ($n_1 = 5$, $n_2 = 11$)	92.462	94.454	94.139	70.021	95.453	54.357
P ($r^2 = 0$, $n_1 = 5$, $n_2 = 11$)	0.000	0.000	0.000	0.000	0.000	0.000
SF contribution	94.3%	91.6%	91.1%	65.5%	66.2%	68.6%
EF contribution	5.7%	8.4%	8.9%	34.5%	33.8%	31.4%

[a] See Table 4 for definition of symbols.

Table 7. CoMFA Models Obtained for 47 Compounds in the Combined Set[a]

|	model 1	model 2	model 3	model 4	model 5	model 6
ONC	5	3	3	5	5	5
r^2_{cv}	0.614	0.683	0.690	0.704	0.688	0.686
PRESS	0.864	0.765	0.756	0.756	0.776	0.779
SEE	0.383	0.476	0.476	0.345	0.356	0.356
r^2	0.924	0.877	0.877	0.938	0.935	0.935
F ($n_1 = 5$, $n_2 = 41$)	99.826	102.414	102.473	125.021	116.995	117.120
P ($r^2 = 0$, $n_1 = 5$, $n_2 = 41$)	0.000	0.000	0.000	0.000	0.000	0.000
SF contribution	91.2%	92.5%	92.0%	60.5%	64.2%	63.3%
EF contribution	8.8%	7.5%	8.0%	39.5%	35.8%	36.7%

[a] See Table 4 for definition of symbols.

usual, increasing the number of the components beyond the minimum necessary to explain the data adds noise in the models. Table 8 lists pK_i values and residuals for each of the 47 molecules. The mean value for residuals in Table 8 is 0.38.

An important observation of CoMFA calculations was made by Tropsha and his student.[62] They found that the CoMFA model and associated statistics for a set of aligned molecules are sensitive to their orientation with respect to the Cartesian coordinate system. To determine the sensitivity for our set of 47 compounds, CoMFA models were computed for over 100 arbitrary orientations. The results are shown in Figure 6. The mean value of r_{cv}^2 is 0.701; the median is 0.697; the minimum is 0.564; the maximum is 0.803. Thus, the value of r_{cv}^2 we presented for the initial orientation appears to be representative of a wider sampling of orientations.

Discussion

To test the robustness of the 47-compound CoMFA model, we evaluated four arylpiperazine antagonists not in the training set: quipazine (**14**), N-methylquipazine (NMQ, **20**), 4-Ph-NMQ (**21**), and KB-6933 (**22**). In each case, the new structure was built on the computer by modifying a closely related structure in the training set.
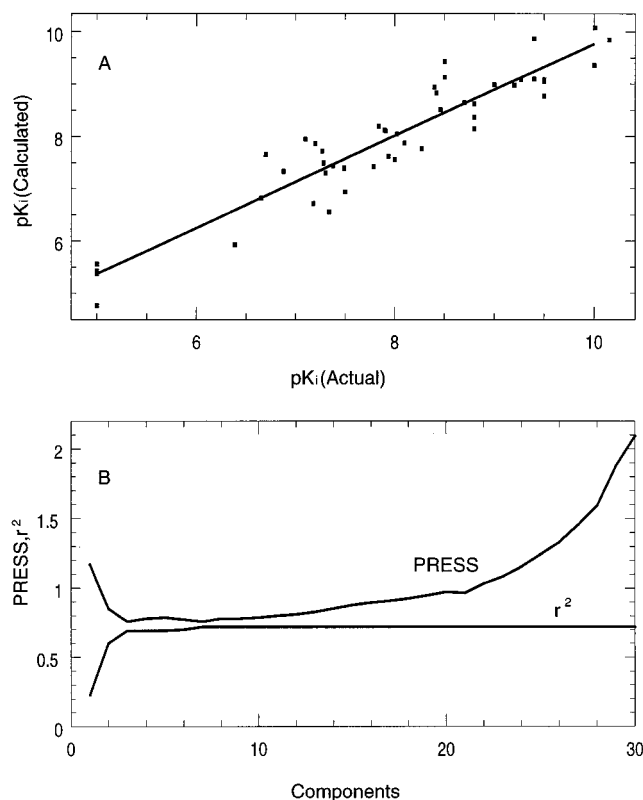
Figure 5. Upper graph: pK_i values calculated with model 3 of Table 7 vs actual values. Lower graph: evolution of PRESS and r^2_{cv} as the number of PLS components increases.

The new structure was not energy-minimized to avoid disturbing the alignment with the CoMFA model. Charges for the new structure were obtained by single-point AM1/SM2 calculations.
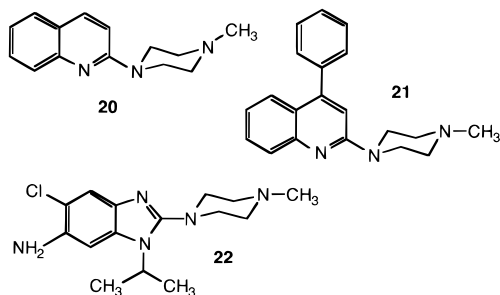

Two experimental pK_i values for quipazine (**14**) have been reported: 8.92[29] and 8.70.[31] The value for quipazine predicted by CoMFA model 3 of Table 7 is 7.28, giving residuals of 1.64 and 1.42, respectively. NMQ (**20**) is predicted more accurately with a residual value of only 0.26 (8.26 predicted vs 8.52 experimentally[31]). To make these CoMFA predictions, the structures of **14** and **20** were constructed from **18f** by replacing the ethyl and methyl side chains (a and b in **18**) with hydrogens; in the case of **14**, the terminal methyl on the piperazine ring was also replaced by hydrogen.

To test the dependence of the predictivity on the number of structural changes, three different starting structures, **16b,f,j**, were chosen for building the 4-Ph-NMQ molecule (**21**). In other words, **21** can be constructed on the computer by modification of any of these different structures in the training set. Three different pK_i values are predicted: 8.15, 8.21, and 8.47. These

Table 8. Actual and CoMFA-Predicted Affinities (pK_i) and Residuals for Each of the 47 5-HT₃ Receptor Antagonists in the Combined Set

molecule	actual	predicted	residual
16a	7.49	7.39	0.10
16b	7.90	8.12	−0.22
16c	7.28	7.49	−0.21
16d	6.39	5.93	0.46
16e	7.94	7.62	0.32
16f	8.80	8.36	0.44
16g	7.27	7.72	−0.45
16h	5.00	5.56	−0.56
16i	7.91	8.10	−0.19
16j	8.42	8.83	−0.41
16k	7.84	8.19	−0.35
16l	7.34	6.56	0.78
16m	8.27	7.77	0.50
16n	8.46	8.51	−0.05
16o	8.10	7.87	0.23
16p	5.00	5.38	−0.38
17a	6.88	7.33	−0.45
17b	8.02	8.04	−0.02
17c	7.79	7.42	0.37
17d	5.00	5.43	−0.43
17e	7.18	6.72	0.46
17f	7.38	7.44	−0.06
17g	6.65	6.82	−0.17
17h	5.00	4.76	0.24
18a	10.15	9.85	0.30
18b	10.00	9.36	0.64
18c	10.01	10.08	−0.07
18d	9.40	9.87	−0.47
18e	8.50	9.43	−0.93
18f	9.27	9.09	0.18
19a	7.30	7.30	0.00
19b	7.10	7.94	−0.84
19c	8.00	7.56	0.44
19d	8.80	8.15	0.65
19e	9.20	8.98	0.22
19f	9.50	9.08	0.42
19g	9.50	9.05	0.45
19h	8.80	8.62	0.18
19i	7.20	7.86	−0.66
19j	9.50	8.77	0.73
19k	8.40	8.94	−0.54
19l	9.00	8.99	0.01
19m	6.70	7.65	−0.95
19n	9.40	9.10	0.30
19o	8.70	8.64	0.06
19p	8.50	9.13	−0.63
19q	7.50	6.94	0.56
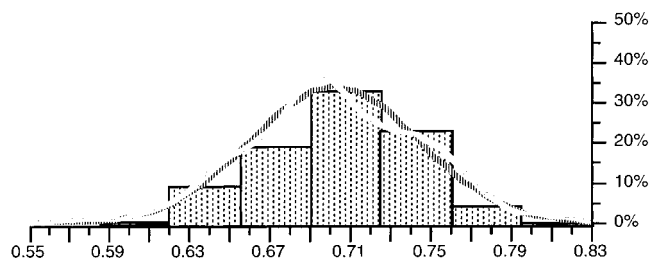
Figure 6. Histogram showing the distribution of r_{cv}^2 values obtained for the 47-compound set in 103 orientations with respect to the Cartesian coordinate system. The set of aligned molecules was rotated in 30° increments about the x, y, and z axes starting from the initial orientation and from an orientation offset 45° from the initial one. The vertical scale shows the percentage of the values that fall in each of the intervals indicated on the horizontal scale. A normal distribution curve (hashed) is superposed on the data; the gray curve is smoothed to the data according to the nonparametric density estimation method in JMP 3.1.5, a statistical analysis program.

can be compared to the experimental value of 8.47. The variability in predictions gives another indication of the degree of robustness of the CoMFA model. When fewer structural modifications have to be made to convert a
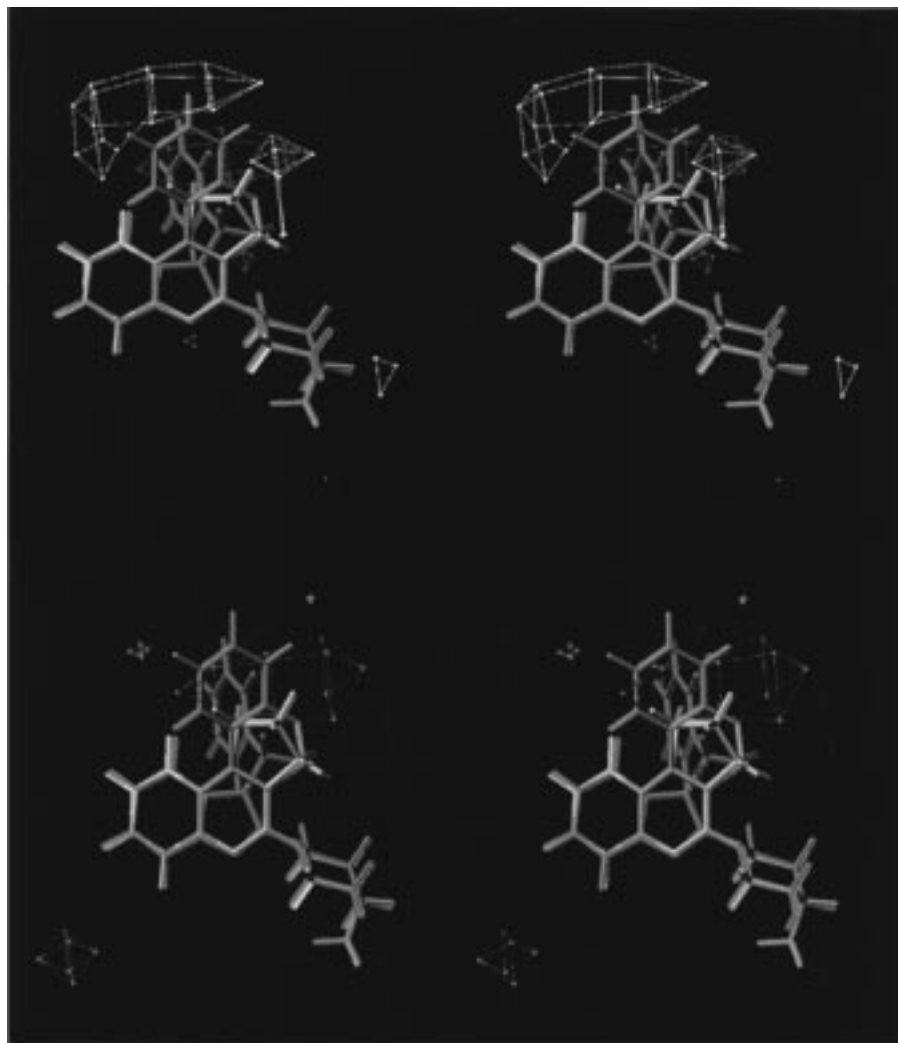
Figure 7. Relaxed stereoview of the CoMFA contours for the 47 5-HT$_3$ receptor antagonists. The steric field map is shown on the top panel and electrostatic on the bottom panel. Contouring levels are at the default values of 80% and 20%. To show more clearly the spatial relationship of the contours, one of the more active compounds in each of the three sets is also displayed: **16f** (orange) from set A, **18a** (white) from set C, and **19e** (cyan) from set O.

structure in the training set to the structure to be predicted, better results (lower residual values) are obtained.

Compound KB-6933 molecule has been reported to be one of the more potent 5-HT$_3$ receptor antagonists with a pK_i value similar to that of the most potent compound in the set of 47. Our prediction for KB-6933, which was built from **19q**, is 9.14 vs 10.18 experimentally.[26] Overall for the four test compounds not in the training set, the mean deviation between experimental and predicted binding affinities is 0.7(±0.7) log unit.

The equations produced from a PLS analysis can contain large numbers of coefficients, so the usual way to visualize CoMFA results is through contour maps of the PLS coefficients. These maps show regions where differences in molecular fields are associated with differences in biological activity. The maps do not show what is common to all molecules of a set, and hence one cannot expect to generate a complete image of the receptor. Indeed, it is becoming better recognized that not all ligands, even similar ones, dock at the same spot in a given receptor.[33] The contour plots, however, do give a direct visual indication of which parts of the molecules differentiate the activities of the compounds in the set under study. The plots also offer an inter-

pretation of how to design new molecules which will have higher binding affinity.

Figure 7 shows the steric (top panel) and electrostatic (bottom panel) contour maps deduced for the 47 compounds using model 3 (Table 7). The color code is as follows: the steric features are green (more bulk increases bioactivity) and yellow (bulkier substituents decrease bioactivity), and the electrostatic features are red (more negative charge increases bioactivity) and blue (the same but for positive charge).

A constant feature of all 5-HT$_3$ antagonists is a basic nitrogen atom. In our set of 47 compounds, there is not much diversity around the distal piperazine nitrogen (only hydrogen, methyl, and ethyl are represented). The contour plots indicate there is steric hindrance near the equatorial position of the piperazine nitrogen and that an increase in pK_i values can be achieved with more positive charge in the axial position (as indicated by the blue cloud in that region). Considering these ideas, we introduced some modifications on three of the more active molecules cited above and predicted the qualitative effect on the pK_i of these hypothetical structures. Substitution at the equatorial position on the terminal piperazine nitrogen of **16e**, **18a**, and **19e** by Me, Et, Pr, *i*-Pr, or *t*-Bu produces, as expected, a decrease in pK_i
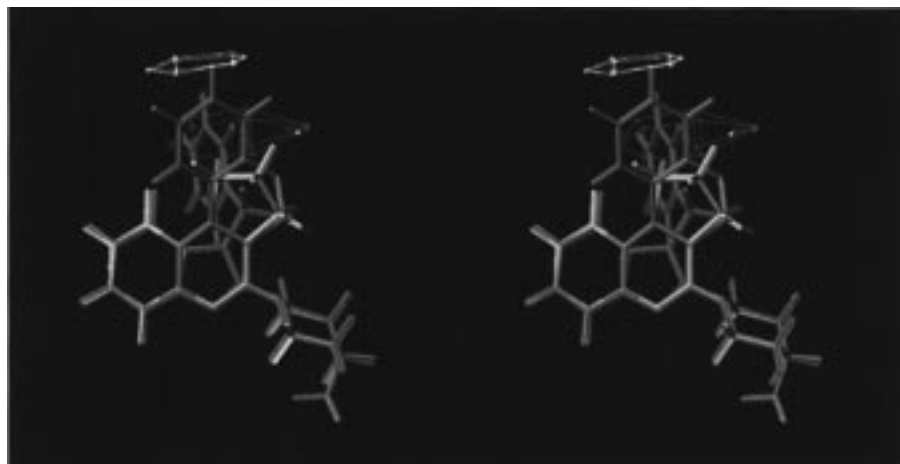
Figure 8. Relaxed stereoview of the CoMFA contours of the steric and electrostatic fields at the 90% and 10% levels.

values, but even with the bulkiest one, the predicted decrease is not drastic. Substitution at the axial position by $-CH_2-NH_2$, $-CH_2-NH_3^+$, $-(CH_2)_2-NH_3^+$, $-CH(CH_3)NH_2$, $-CH(CH_3)NH_3^+$, $-(CH_2)_3-NH_3^+$, or $-(CH_2)_4-NH_3^+$ increases (improves) the pK_i values, and the charged substituents increase pK_i values more than the neutral ones.

As mentioned, CoMFA is unable to correlate bioactivity with a region where all the compounds have minor structural variation. A similar problem was reported by Argarwal et al.[62] in their study of 5-HT$_{1A}$ and 5-HT$_2$ ligands. The steric requirements around the basic nitrogen of 5-HT$_3$ antagonists have not been extensively studied, at least in terms of published experimental pK_i values. Monge et al.[63] studied different substitutions on this nitrogen in piperazinylquinoxaline derivatives, and the more potent compounds were those with limited chain length such as Et or Pr. The work of Anzini et al.[27] showed that a methyl substituent appears to be optimal for interaction with the 5-HT$_3$ receptor. Hori et al.[26] found a decrease in the activity of benzimidazole derivatives when Me is replaced by Et, Pr, or CH$_2$Ph.

Turning to the region of the substituents on the phenyl ring of the benzimidazoles, the electrostatic contour plot on the set of 47 compounds shows only a small red region (indicating an increase of bioactivity should result from extra negative charge) between positions 4 and 5 of the benzimidazole ring. This region may explain why **19f** (with a fluoro substituent) is more active than **19i** (with OMe), which displays positive charge through the hydrogens toward the red region, but does not explain the relative differences in activity of **19g** (with Cl), **19h** (with Me), and **19j** (with OH).

If there is one part in the molecular structure of the combined set where the compounds display the most structural diversity, it is the "top" portion of the heteroaromatic ring. As we can see from the contour plots, this region is rich with CoMFA contours, and some interesting conclusions can be derived from these. The steric plot shows two well-defined regions: a green one close to the $-CH_2Ph$, which is a characteristic substituent in the O set, and a yellow region close to the fused heteroaromatic rings characteristic of the A and C sets. Bioactivity increases with bulkier substituents in the volume occupied by the $-CH_2Ph$ substituent, something commonly found.[13,26-30]

The CoMFA modeling suggests a limitation in the size of the substituents on the fused aromatic rings. It seems that the limitation is imposed by set A as it can be inferred from the yellow cloud enveloping this aromatic region. The more active compounds in the combined set are those synthesized by Castan et al.[30] The electrostatic field plot presents two types of regions: a red one close to the $-CH_2Ph$ substituent and three blue lobes surrounding the fused rings. We used the most active compound (**18a**) to design hypothetical modifications according to this plot. First, the methylene of carbon atom b (see structure in Table 2) was substituted by an oxygen, and the predicted pK_i value decreases slightly (9.67 vs 9.85 for **18a** in Table 8). Substitution of both hydrogens on carbon b by two chlorine atoms leaves the pK_i value essentially unchanged (9.87 vs 9.85). When only one hydrogen is substituted by chloro, a chiral center appears. The *S*-enantiomer increases the pK_i value (10.20 vs 9.85), whereas the *R*-enantiomer decreases the value (9.54 vs 9.85) as could be expected. Within the realm of structures that seemed within the scope of our CoMFA model, we found no new structures with significantly better predicted binding affinity than those compounds already reported in the literature.

Finally, Figure 8 shows the CoMFA contour plot for model 3 (Table 7) but using 90% and 10% contouring levels instead of the default 80% and 20%. By comparing Figures 7 and 8, the regions most strongly influencing the bioactivity can be seen. These influential regions are localized in the "top" part of the molecular set.

A thorough investigation of the effect of different ways of calculating charges in the CoMFA results has been reported recently for a set of 37 benzodiazepine receptor ligands.[57] Kroemer et al. concluded that a good compromise between computational effort and quality of results can be achieved with electrostatically fit charges from semiempirical molecular orbital theory. Overall, our results were not highly sensitive to the method used to compute charges, perhaps because of the dominance of the steric field in almost all cases.

In conclusion, a fairly robust CoMFA model has been obtained for the combined set of 47 arylpiperazines that bind to the 5-HT$_3$ receptor. On the other hand, poor models were found for two of the smaller subsets. With the other subset (set A), we obtain somewhat better results than previously reported[29] perhaps because of using the *d*-tubocurarine structure as a template for conformational alignment. By using a large training

set of compounds, our analysis yielded a CoMFA model with reasonably good demonstrated predictivity. As additional arylpiperazines with antagonistic 5-HT$_3$ activity are reported in the literature, further insights into the requirements for bioactivity can be obtained.[64]

References

(1) Aprison, M. H.; Gálvez-Ruano, E.; Lipkowitz, K. B. Comparison of Binding Mechanisms at Cholinergic, Serotonergic, Glycinergic and GABAergic Receptors. *J. Neurosci. Res.* **1996**, *43*, 127–136. A preliminary molecular alignment for 5-HT$_3$ was given in this paper, but it has subsequently been revised; see: Gálvez-Ruano, E.; Iriepa, I.; Morreale, A. Natural Templates for the Nervous System Receptor Ligands. I. Competitive Antagonist Alkaloids at the Glycinergic, GABAergic, Cholinergic, and Serotonergic Receptors. *Trends Heterocycl. Chem.* **1997**, *5*, 135–144.

(2) Butler, A.; Hill, J. M.; Ireland, S. J.; Jordan, C. C.; Tyers, M. B. Pharmacological Properties of GR 38023F, A Novel Antagonist at 5-HT$_3$ Receptors. *Br. J. Pharmacol.* **1988**, *94*, 397–412.

(3) Bermudez, J.; Fake, C. S.; Joiner, G. F.; Joiner, K. A.; King, F. D.; Miner, W. D.; Sanger, G. J. 5-Hydroxytryptamine (5-HT$_3$) Receptor Antagonists. 1. Indazole and Indolizine-3-carboxylic Acid Derivatives. *J. Med. Chem.* **1990**, *33*, 1924–1929.

(4) Richardson, B. P.; Engel, G.; Donatsch, P.; Stadler, P. A. Identification of Serotonin M-Receptor Subtypes and Their Specific Blockade by a New Class of Drugs. *Nature* **1985**, *316*, 126–131.

(5) See, e.g.: Whelan, B. A.; Iriepa, I.; Gálvez, E.; Orjales, A.; Berisa, A.; Labeaga, L.; García, A.; Uceda, G.; Sanz-Aparicio, J.; Fonseca, I. Synthesis and Structural, Conformational, Biochemical, and Pharmacological Study of New Compounds Derived from Tropane-3-spiro-4′(5′)-imidazoline as Potential 5-HT$_3$ Antagonists. *J. Pharm. Sci.* **1995**, *84*, 101–106.

(6) Robertson, D. W.; Lacefield, W. D.; Bloomquist, W.; Pfeifer, W.; Simon, R. L.; Cohen, M. L. Zatosetron, A Potent, Selective, and Long-Acting 5-HT$_3$ Receptor Antagonist: Synthesis and Structure–Activity Relationships. *J. Med. Chem.* **1992**, *35*, 310–319.

(7) Fozard, J. R. MDL 72222: A Potent and Highly Selective Antagonist at Neuronal 5-Hydroxytryptamine Receptors. *Naunyn-Schmiedeberg's Arch. Pharmacol.* **1984**, *326*, 36–44.

(8) Ohta, M.; Suzuki, K.; Furuya, T.; Kurihara, H.; Tokunaga, T.; Miyata, K.; Yanagisawa, I. Novel 5-Hydroxytryptamine (5-HT$_3$) Receptor Antagonists. III. Pharmacological Evaluations and Molecular Modeling Studies of Optically Active 4,5,6,7-Tetrahydro-1*H*-benzimidazole Derivatives. *Chem. Pharm. Bull.* **1996**, *44*, 1707–1716.

(9) Kawakita, T.; Kuroita, T.; Yasumoto, M.; Sano, M.; Inaba, K.; Fukuda, T.; Tahara, T. Synthesis and Pharmacology of 3,4-Dihydro-3-oxo-1,4-benzoxazine-8-carboxamide Derivatives, A New Class of Potent Serotonin-3 (5-HT$_3$) Receptor Antagonists. *Chem. Pharm. Bull.* **1992**, *40*, 624–630.

(10) Volonté, M.; Ceci, A.; Borsini, F. Effect of the 5-Hydroxytryptamine$_3$ Receptor Antagonist Itasetron (DAU 6215) on (+)-*N*-Allylnormetazocina-Induced Dopamine Release in the Nucleus Accumbens and in the Corpus Striatum of the Rat: An In Vivo Microdialysis Study. *J. Pharmacol. Exp. Ther.* **1995**, *275*, 358–367.

(11) van Wijngaarden, I.; Hamminga, D.; van Hes, R.; Standaar, P. J.; Tipker, J.; Tulp, M. Th. M.; Mol, F.; Olivier, B.; de Jonge, A. Development of High-Affinity 5-HT$_3$ Receptor Antagonists. Structure-Affinity Relationships of Novel 1,7-Annelated Indole Derivatives. 1. *J. Med. Chem.* **1993**, *36*, 3693–3699.

(12) Smith, W. W.; Sancilio, L. F.; Owera-Atepo, J. B.; Naylor, R. J.; Lambert, L. Zacopride, A Potent 5-HT$_3$ Antagonist. *J. Pharm. Pharmacol.* **1988**, *40*, 301–302.

(13) Orjales, A.; Mosquera, R.; Labeaga, L.; Rodes, R. New 2-Piperazinylbenzimidazole Derivatives as 5-HT$_3$ Antagonists. Synthesis and Pharmacological Evaluation. *J. Med. Chem.* **1997**, *40*, 586–593.

(14) Gupta, S. K.; Kunka, R. L.; Metz, A.; Lloyd, T.; Rudolph, G.; Perel, J. M. Effect of Alosetron (a New 5-HT$_3$ Receptor Antagonist) on the Pharmacokinetics of Haloperidol in Schizophrenic Patients. *J. Clin. Pharmacol.* **1995**, *35*, 202–207.

(15) King, F. D.; Jones, J. B.; Sanger, G. J. *5-Hydroxytryptamine-3 Receptor Antagonists*; CRC Press: Boca Raton, FL, 1994.

(16) Hibert, M. F.; Hoffmann, R.; Miller, R. C.; Carr, A. A. Conformation-Activity Relationship Study of 5-HT$_3$ Receptor Antagonists and a Definition of a Model for This Receptor Site. *J. Med. Chem.* **1990**, *33*, 1594–1600.

(17) Swain, C. J.; Baker, R.; Kneen, C.; Herbert, R.; Moseley, J.; Saunders, J.; Seward, E. M.; Stevenson, G. I.; Beer, M.; Stanton, J.; Watling, K.; Ball, R. G. Novel 5-HT$_3$ Antagonists: Indol-3-ylspiro(azabicycloalkane-3,5′(4′*H*)-oxazoles). *J. Med. Chem.* **1992**, *35*, 1019–1031.

(18) Hibert, M. F. Molecular Modeling Studies of the 5-HT$_3$ Antagonist Recognition. In *5-Hydroxytryptamine-3 Receptor Antagonists*; King, F. D., Jones, J. B., Sanger, G. J., Eds.; CRC Press: Boca Raton, FL, 1994; pp 45–66.

(19) Laguerre, M.; Dubost, J.-P.; Kummer, E.; Carpy, A. Molecular Modeling of the 5-HT$_3$ Receptor Antagonists: Geometrical, Electronic and Lipophilic Features of the Pharmacophore and 3D-QSAR Study. *Drug Des. Discovery* **1994**, *11*, 205–222. See also: Dubost, J.-P. 2D and 3D Lipophilicity Parameters in QSAR. In *Trends in QSAR and Molecular Modeling 92*; Wermuth, C. G., Ed.; ESCOM: Leiden, 1993; pp 93–100.

(20) Bureau, R.; Lancelot, J. C.; Pruier, H.; Rault, S. Conformational Analysis and 3D QSAR Study on Novel Partial Agonists of 5-HT$_3$ Receptors. *Quant. Struct.-Act. Relat.* **1996**, *15*, 373–381.

(21) Heidempergher, F.; Pillan, A.; Pinciroli, V.; Vaghi, F.; Arrigoni, C.; Bolis, G.; Caccia, C.; Dho, L.; McArthur, R.; Varasi, M. Phenylimidazolidin-2-one Derivatives as Selective 5-HT$_3$ Receptor Antagonists and Refinement of the Pharmacophore Model for 5-HT$_3$ Receptor Binding. *J. Med. Chem.* **1997**, *40*, 3369–3380. These authors hypothesized that the first component, the aromatic ring, may play the role of only a spacer, whereas most other authors consider interactions of a delocalized π-electron system and the receptor important.

(22) Rosen, T.; Nagel, A. A.; Rizzi, J. P.; Ives, J. L.; Daffeh, J. B.; Ganong, A. H.; Guarino, K.; Heym, J.; McLean, S.; Nowakowski, J. T.; Schmidt, A. W.; Seeger, T. F.; Siok, C. J.; Vincent, L. A. Thiazole as a Carbonyl Bioisostere. A Novel Class of Highly Potent and Selective 5-HT$_3$ Receptor Antagonists. *J. Med. Chem.* **1990**, *33*, 2715–2720.

(23) Round, A.; Wallis, D. I. Further Studies on the Blockade of 5-HT Depolarizations of Rabbit Vagal Afferent and Sympathetic Ganglion Cells by MDL 72222 and Other Antagonists. *Neuropharmacology* **1987**, *26*, 39–48.

(24) Emerit, M. B.; Riad, M.; Fattaccini, C. M.; Hammon, M. Characteristics of [14C]Guanidinium Accumulation in NG 108-15 Cells Exposed to Serotonin 5-HT$_3$ Receptor Ligands and Substance P. *J. Neurochem.* **1993**, *60*, 2059–2067.

(25) Glennon, R. A.; Ismaiel, A. E. M.; McCarthy, B. G.; Peroutka, S. J. Binding of Arylpiperazines to 5-HT$_3$ Serotonin Receptors: Results of a Structure-Affinity Study. *Eur. J. Pharmacol.* **1989**, *168*, 387–392.

(26) Hori, M.; Suzuki, K.; Yamamoto, T.; Nakajima, F.; Ozaki, A.; Ohtaka, H. Design and Synthesis of a Series of Novel Serotonin$_3$ Antagonists. *Chem. Pharm. Bull.* **1993**, *41*, 1832–1841. See also: Ohtaka, H.; Fujita, T. Structural Modification Patterns from Agonist to Antagonists and Their Application to Drug Design – A New Serotonin (5-HT$_3$) Antagonist Series. In *Progress in Drug Research*; Jucker, E., Ed.; Birkhäuser Verlag: Basel, 1993; Vol. 41, pp 313–357.

(27) Anzini, M.; Cappelli, A.; Vomero, S.; Cagnotto, A.; Skorupska, M. 6-(1-Piperazinyl)-7*H*-indeno[2,1-*c*]quinoline Derivatives with High Affinity and Selectivity for 5-HT$_3$ Serotonin Sites. *Med. Chem. Res.* **1993**, *3*, 44–51.

(28) Monge, A.; Peña, M. del C.; Palop, J. A.; Calderó, J. M.; Roca, J.; García, E.; Romero, G.; Del Río, J.; Lasheras, B. Synthesis of 2-Piperazinylbenzothiazole and 2-Piperazinylbenzoxazole Derivatives with 5-HT$_3$ Antagonist and 5-HT$_4$ Agonist Properties. *J. Med. Chem.* **1994**, *37*, 1320–1325.

(29) Anzini, M.; Cappelli, A.; Vomero, S.; Giorgi, G.; Langer, T.; Hamon, M.; Merahi, N.; Emerit, B. M.; Cagnotto, A.; Skorupska, M.; Mennini, T.; Pinto, J. C. Novel, Potent, and Selective 5-HT$_3$ Receptor Antagonists Based on the Arylpiperazine Skeleton: Synthesis, Structure, Biological Activity, and Comparative Molecular Field Analysis Studies. *J. Med. Chem.* **1995**, *38*, 2692–2704.

(30) Castan, F.; Schambel, P.; Enrici, A.; Rolland, F.; Bigg, D. C. H. New Arylpiperazine Derivatives with High Affinity for 5-HT$_3$ Receptor Sites. *Med. Chem. Res.* **1996**, *6*, 81–101.

(31) Dukat, M.; Abdel-Rahman, A. A.; Ismaiel, A. E. M.; Ingher, S.; Teitler, M.; Gyermek, L.; Glennon, R. A. Structure–Activity Relationships for the Binding of Arylpiperazines and Arylbiguanides at 5-HT$_3$ Serotonin Receptors. *J. Med. Chem.* **1996**, *39*, 4017–4026.

(32) Greco, G.; Novellino, E.; Martin, Y. C. Approaches to Three-Dimensional Quantitative Structure–Activity Relationships. In *Reviews in Computational Chemistry*; Lipkowitz, K. B., Boyd, D. B., Eds.; Wiley-VCH: New York, 1997; Vol. 11, pp 127–182.

(33) Oprea, T. I.; Waller, C. L. Theoretical and Practical Aspects of Three-Dimensional Quantitative Structure−Activity Relationships. In *Reviews in Computational Chemistry*; Lipkowitz, K. B., Boyd, D. B., Eds.; Wiley-VCH: New York, 1997; Vol. 11, pp 183−240.

(34) Cramer, R. D., III; Patterson, D. E.; Bunce, J. D. Comparative Molecular Field Analysis (CoMFA). 1. Effect of Shape on Binding of Steroids to Carrier Proteins. *J. Am. Chem. Soc.* **1988**, *110*, 5959−5967.

(35) Cramer, R. D., III; DePriest, S. A.; Patterson, D. E.; Hecht, P. The Developing Practice of Comparative Molecular Field Analysis. In *3D-QSAR in Drug Design: Theory, Methods and Applications*; Kubinyi, H., Ed.; ESCOM: Leiden, 1993; pp 443−485.

(36) Martin, Y. C.; Kim, K. H.; Lin, C. T. Comparative Molecular Field Analysis: CoMFA. In *Advances in Quantitative Structure−Property Relationships*; Charton, M., Ed.; JAI Press: Greenwich, CT, 1996; Vol. 1, pp 1−52.

(37) CoMFA analyses have been done on other arylpiperazines that bind to other serotonin receptors. See, e.g.: Lopez-Rodriguez, M. L.; Rosado, M. L.; Benhamu, B.; Morcillo, M. J.; Fernandez, E.; Schaper, K. J. Synthesis and Structure−Activity Relationships of a New Model of Arylpiperazines. 2. Three-Dimensional Quantitative Structure−Activity Relationships of Hydantoin-phenylpiperazine Derivatives with Affinity for 5-HT₁ₐ and α₁ Receptors. A Comparison of CoMFA Models. *J. Med. Chem.* **1997**, *40*, 1648−1656. van Steen, B. J.; van Wijngaarden, I.; Tulp, M. T.; Soudijn, W. Structure-Affinity Relationship Studies on 5-HT₁ₐ Receptor Ligands. 2. Heterobicyclic Phenylpiperazines with N₄-Aralkyl Substituents. *J. Med. Chem.* **1994**, *37*, 2761−2773. Langlois, M.; Bremont, B.; Rousselle, D.; Gaudy, F. Structural Analysis by the Comparative Molecular Field Analysis Method of the Affinity of Beta-adrenoreceptor Blocking Agents for 5-HT₁ₐ and 5-HT₁ᵦ Receptors. *Eur. J. Pharmacol.* **1993**, *244*, 77−87.

(38) Yakel, J. L.; Jackson, M. B. 5-HT₃ Receptors Mediate Rapid Response in Cultured Hippocampus and a Clonal Cell Line. *Neuron* **1988**, *1*, 615−621.

(39) Maksay, G. Distinct Thermodynamic Parameters of Serotonin 5-HT₃ Agonists and Antagonists to Displace [³H]-Granisetron Binding. *J. Neurochem.* **1996**, *67*, 407−412.

(40) Cappelli, A.; Donati, A.; Anzini, M.; Vomero, S.; De Benedetti, P. G.; Menziani, M. C.; Langer, T. Molecular Structure and Dynamics of Some Potent 5-HT₃ Receptor Antagonists. Insight in the Interaction with the Receptor. *Bioorg. Med. Chem.* **1996**, *4*, 1255−1269.

(41) Codding, P. W.; James, M. N. G. The Crystal and Molecular Structure of a Potent Neuromuscular Blocking Agent: *d*-Tubocurarine Dichloride Pentahydrate. *Acta Crystallogr., Sect. B* **1973**, *29*, 935−942.

(42) SYBYL, version 6.1; Tripos Associates, 1699 S. Hanley Rd, Suite 303, St. Louis, MO 63144.

(43) Clark, M.; Cramer, R. D., III; Van Opdenbosch, N. Validation of the General Purpose Tripos 5.2 Force Field. *J. Comput. Chem.* **1989**, *10*, 982−1012.

(44) Leach, A. R. A Survey of Methods for Searching the Conformational Space of Small and Medium-Sized Molecules. In *Reviews in Computational Chemistry*; Lipkowitz, K. B., Boyd, D. B., Eds.; VCH Publishers: New York, 1991; Vol. 2, pp 1−55.

(45) Dewar, M. J. S.; Zoebisch, E. G.; Healy, E. F.; Stewart, J. J. P. AM1: A New General Purpose Quantum Mechanical Molecular Model. *J. Am. Chem. Soc.* **1985**, *107*, 3902−3909. See also: Stewart, J. J. P. Semiempirical Molecular Orbital Methods. In *Reviews in Computational Chemistry*; Lipkowitz, K. B., Boyd, D. B., Eds.; VCH Publishers: New York, 1990; Vol. 1, pp 45−81.

(46) Stewart, J. J. P. MOPAC: A General Molecular Orbital Package. *Quant. Chem. Prog. Exch. Bull.* **1993**, *13*, 40−43. MOPAC version 7.0 (Fujitsu Ltd.) is available as Program 455 from QCPE, Indiana University, Bloomington, IN 47405.

(47) Quanta96; Molecular Simulations, Inc., 9685 Scranton Rd, San Diego, CA 92121.

(48) Brooks, B. R.; Bruccoleri, R. E.; Olafson, B. D.; States, D. J.; Swaminathan, S.; Karplus, M. CHARMM: A Program for Macromolecular Energy, Minimization and Dynamics Calculations. *J. Comput. Chem.* **1983**, *4*, 187−217.

(49) Momany, F. A.; Rone, R. Validation of the General Purpose QUANTA3.2/CHARMm Force Field. *J. Comput. Chem.* **1992**, *7*, 888−900.

(50) Schlick, T. Optimization Methods in Computational Chemistry. In *Reviews in Computational Chemistry*; Lipkowitz, K. B., Boyd, D. B., Eds.; VCH Publishers: New York, 1992; Vol. 3, pp 1−71.

(51) Motoc, I.; Dammkoehler, R. A.; Mayer, D.; Labanowski, J. Three-Dimensional Quantitative Structure−Activity Relationships. I. General Approach to the Pharmacophore Model Validation. *Quant. Struct.-Act. Relat.* **1986**, *5*, 99−105. Labanowski, J.;

Motoc, I.; Naylor, C. B.; Mayer, D.; Dammkoehler, R. A. Three-Dimensional Quantitative Structure−Activity Relationships. 2. Conformational Mimicry and Topographical Similarity of Flexible Molecules. *Quant. Struct.-Act. Relat.* **1986**, *5*, 138−152.

(52) Lin, H.-S.; Rampersaud, A. A.; Zimmerman, K.; Steinberg, M. I.; Boyd, D. B. Nonpeptide Angiotensin II Receptor Antagonists: Synthetic and Computational Chemistry of *N*-[[4-[2-(2*H*-Tetrazol-5-yl)-1-cycloalken-1-yl]phenyl]methyl]imidazole Derivatives and Their In Vitro Activity. *J. Med. Chem.* **1992**, *35*, 2658−2667. Boyd, D. B.; Palkowitz, A. D.; Thrasher, K. J.; Hauser, K. L.; Whitesitt, C. A.; Reel, J. K.; Simon, R. L.; Pfeifer, W.; Lifer, S. L.; Takeuchi, K.; Vasudevan, V.; Kossoy, A. D.; Deeter, J. B.; Steinberg, M. I.; Zimmerman, K. M.; Wiest, S. A.; Marshall, W. S. Molecular Modeling and Quantitative Structure−Activity Relationship Studies in Pursuit of Highly Potent Substituted Octanoamide Angiotensin II Receptor Antagonists. In *Computer-Aided Molecular Design: Applications in Agrochemicals, Materials, and Pharmaceuticals*; ACS Symp. Series 589; Reynolds, C. H., Holloway, M. K., Cox, H. K., Eds.; American Chemical Society: Washington, DC, 1995; pp 14−35.

(53) Cramer, C. J.; Truhlar, D. G. Continuum Solvation Models: Classical and Quantum Mechanical Implementations. In *Reviews in Computational Chemistry*; Lipkowitz, K. B., Boyd, D. B., Eds.; VCH Publishers: New York, 1995; Vol. 6, pp 1−72.

(54) Hehre, W. J.; Burke, L. D.; Shusterman, A. J. *A Spartan Tutorial*; Wavefunction, Inc.: Irvine, CA, 1993. Spartan version 4.1.1 was used.

(55) Alignment was performed with optimized structures in SYBYL, and charges were obtained with the Gasteiger−Hückel method. Once the alignment was performed in this way (models 1 and 4), charges were computed on these geometries with the other theoretical methods (models 2, 3, 5, and 6).

(56) Williams, D. E. Net Atomic Charge and Multipole Models for the Ab Initio Molecular Electric Potential. In *Reviews in Computational Chemistry*; Lipkowitz, K. B., Boyd, D. B., Eds.; VCH Publishers: New York, 1991; Vol. 2, pp 219−271. See also: Francl, M. M.; Chirlian, L. E. The Plusses and Minuses of Mapping Atomic Charges to Electrostatic Potentials. In *Reviews in Computational Chemistry*; Lipkowitz, K. B., Boyd, D. B., Eds.; Wiley-VCH: New York, in press.

(57) Kroemer, R. T.; Hecht, P.; Liedl, K. R. Different Electrostatic Descriptors in Comparative Molecular Field Analysis: A Comparison of Molecular Electrostatic and Coulomb Potentials. *J. Comput. Chem.* **1996**, *17*, 1296−1308.

(58) Geladi, P.; Kowalski, B. R. Partial Least-Squares Regression: A Tutorial. *Anal. Chim. Acta* **1986**, *185*, 1−17.

(59) Höskuldsson, A. PLS Regression Methods. *J. Chemomet.* **1988**, *2*, 211−228.

(60) Ståhle, L.; Wold, S. Multivariate Data Analysis and Experimental Design in Biomedical Research. In *Progress in Medicinal Chemistry*; Ellis, G. P., West, G. B., Eds.; Elsevier Science Publishers: Amsterdam, 1988; Vol. 25, pp 291−338.

(61) Argarwal, A.; Pearson, P. P.; Taylor, E. W.; Li, H. B.; Dahlgren, T.; Herslöf, M.; Yang, Y.; Lambert, G.; Nelson, D. L.; Regan, J. W.; Martin, A. R. Three-Dimensional Quantitative Structure−Activity Relationships of 5-HT Receptor Binding Data for Tetrahydropyridinylindole Derivatives: A Comparison of the Hansch and CoMFA Methods. *J. Med. Chem.* **1993**, *36*, 4006−4014.

(62) Cho, S. J.; Tropsha, A. Cross-Validated R²-Guided Region Selection for Comparative Molecular Field Analysis: A Simple Method To Achieve Consistent Results. *J. Med. Chem.* **1995**, *38*, 1060−1066.

(63) Monge, A.; Palop, J. A.; Del Castillo, J. C.; Calderó, J. M.; Roca, J.; Romero, G.; Del Río, J.; Lasheras, B. Novel Antagonists of 5-HT₃ Receptors. Synthesis and Biological Evaluation of Piperazinylquinoxaline Derivatives. *J. Med. Chem.* **1993**, *36*, 2745−2750.

(64) After our paper had been submitted for publication, additional relevant papers appeared. One shows a diversity of aromatic ring systems in a pharmacophoric alignment; see: Rival, Y.; Hoffmann, R.; Didier, B.; Rybaltchenko, V.; Bourguignon, J.-J.; Wermuth, C. G. 5-HT₃ Antagonists Derived from Aminiopyridazine Muscarinic M1 Agonists. *J. Med. Chem.* **1998**, *41*, 311−317. A second paper shows that regression-type QSARs can be obtained with theoretical descriptors if outlying 5-HT₃ antagonists are neglected, but no multiple regression analyses were reported by Cappelli, A.; Anzini, M.; Vomero, S.; Mennuni, L.; Makovec, F.; Doucet, K.; Hamon, M.; Bruni, G.; Romero, M. R.; Menziani, M. C.; De Benedetti, P. G.; Langer, T. Novel Potent and Selective Central 5-HT₃ Receptor Ligands Provided with Different Intrinsic Efficacy. 1. Mapping the Central 5-HT₃ Receptor Binding Site by Arylpiperazine Derivatives. *J. Med. Chem.* **1998**, *41*, 728−741.